GROWTH OF NATURALLY INITIATED FATIGUE CRACKS IN ALLOY 800 UNDER SYMMETRICAL PUSH-PULL LOADING

R. Adolfs*, H.-J. Christ* and K. Detert*

The fatigue behaviour of Alloy 800 H has been analysed with special emphasis on the description of the propagation of short cracks. Low-cycle fatigue tests were performed by symmetrical push-pull loading of shallow-notched specimens. The growth of naturally initiated cracks was monitored using a replica technique. The experimental crack growth data were applied to the model of Navarro et al.. for growth of short fatigue cracks which tries to take the influence of microstructural barriers such as grain boundaries into account. The cyclic lifetimes at different stress levels could be assessed by integrating the crack growth equation. The comparison with the experimental results showed reasonable agreement. Only at high numbers of cycles to fracture major deviations in the sense of a conservative prediction were observed.

INTRODUCTION

Fatigue life of components can be divided into the stages nucleation and development of cracks to a length up to a microstructural unit size and short to long (macro-)crack propagation (up to a critical crack length) resulting in the final failure of the component (1). The number of cycles spent to initiate a microcrack depends on the applied load. Under low-cycle fatigue (LCF) conditions cracks are usually formed during a small fraction of the total life. Therefore, under these conditions crack nucleation can often be neglected assuming that small defects acting as cracks are already present at the beginning of the lifetime. Consequently, the main part of lifetime is spent during crack propagation. In most cases cracks are initiated on the surface and are first contained within a single grain. Characterization of propagation behaviour of short cracks is difficult because of their three-dimensional nature, the coalescence of cracks and the effect of microstructure, e.g. grain boundaries and inclusions, which may lead to accelerated or retarded growth rates.

* Institut für Werkstofftechnik, Universität-GH-Siegen
D-57068 Siegen, Fed. Rep. Germany

A simple model proposed by Navarro et al. (2-4) can be considered as a first approach to take at least the existence of grain boundaries into account. The capability of this model for describing the propagation behaviour of short fatigue cracks is critically examined by applying the model to experimental data observed on Alloy 800 H.

EXPERIMENTAL PROCEDURE

The results reported here have been obtained as part of an extensive study on three different age-hardened alloys. For the sake of clarity, the following presentation is restricted to the austenitic steel Alloy 800 H in a relatively soft condition which was achieved by annealing for one hour at 960°C resulting in a mean grain size of 140 μm (excluding twin boundaries).

Low-cycle fatigue tests were performed in air at room temperature under symmetrical push-pull conditions (R_ε=-1) in total strain control with constant strain amplitude ranging from 0.18% to 1.5%. For this purpose a specimen geometry with a cylindrical gauge length of 8 mm diameter and a length of 25 mm was used. Prior to testing all samples were polished. The tests were run till failure which was defined as a 20 percent reduction of peak force in tension.

In order to study the natural initiation and propagation of cracks, shallow-notched specimens which are shown schematically in Fig. 1 were cyclically loaded at different stress amplitude levels and a replica technique was applied. A thin foil of 0.08 mm thickness wetted with acetone was used to take replicas from the whole notch root at regular intervals. The replicas were examined by means of an optical microscope and the observed cracks were studied and characterized.

CRACK PROPAGATION MODEL

The experimental crack data were applied to a model describing the propagation of short cracks which has been proposed by Navarro and De Los Rios (2-4). This model tries to take the influence of microstructural barriers to crack propagation such as grain boundaries and inclusions into account. For this purpose it is assumed that the crack is initiated by a shear mechanism along a slip plane or slip band within a single grain and is constrained by the surrounding grain boundaries. The plasticity is proposed to be localized within the slip band. Furthermore, the crack growth rate *dl/dN* is assumed to be proportional to the crack tip plastic displacement ϕ according to the equation

$$\frac{dl}{dN} = f\,\phi \tag{1}$$

The parameter f therefore defines the part of the plastic displacement at the crack tip which is converted into crack growth. As schematically represented in Fig. 2, the slip band is blocked by grain boundaries or other microstructural barriers acting as obstacles. This leads to a deceleration in growth rate as the crack tip approaches the barrier. A critical condition is fulfilled if the stress concentration at the obstacle is sufficiently high to expand the slip band into the neighbouring grain. Then the crack growth rate accelerates spontaneously. This process is repeated grain after grain until the intermittent crack growth dampens its oscillations as the crack becomes longer. Finally, a transition from short to long crack behaviour is reached, the oscillations cease and a monotonic increase in crack growth rate follows.

The crack tip plastic displacement ϕ can be calculated directly as a function of crack length according to the equations derived and explained in detail by Navarro et al. (2,3). For this purpose several material parameter such as grain size, UTS, fatigue limit and shear modulus must be known.

RESULTS AND DISCUSSION

The cyclic deformation behaviour of Alloy 800H in the condition considered here is characterized by a short initial region of cyclic hardening which is followed by a pronounced cyclic saturation state. It can be concluded in accord with earlier work (e.g. 5,6) that a stable microstructural state is easily established during cycling and that no particle strengthening due to γ' precipitates exists. The evaluation of the LCF data obtained on unnotched specimens (7) provides important input data for the crack propagation model.

In Fig. 3 the result of a crack propagation test at a strain amplitude of 0.11% is shown in a representation of the crack growth rate as a function of the surface crack length. Furthermore, the crack path and the positions of the grain boundaries are illustrated by means of an optical micrograph. Macroscopically the crack grows perpendicularly to the stress axis (vertical in Fig. 3), but microscopically the growth direction is strongly affected by the microstructure. The effect of grain boundaries and changing crystallographic orientations lead to a zigzag path of the crack and marked fluctuations in the crack growth rate.

A comparision between calculated (solid lines) and observed crack growth rates (data points) is shown in Fig. 4 for the example of a stress amplitude of 228 MPa. The lower curve represents the prediction of the minimum crack growth rate which corresponds to a crack approaching a grain boundary, whereas the upper curve is connected with a crack which just has overcome the obstacle and now propagates with a maximum crack growth rate. It should be noted that the factor f (see Eq. 1) serves as a fitting parameter in the model and that its value was adapted numerically by comparing the calculated crack tip plastic displacement with the experimentally observed crack growth rates. Test data located outside the predicted curves point out the differences between the real microstructure and the simplifying model assumptions.

In order to estimate the number of cycles required to grow a crack up to a typical length at failure (4mm), the crack growth equation of the model was integrated applying the procedure explained in detail in (2). The calculation was carried out on the basis of the stress amplitudes used in the LCF tests. A comparison between the predicted and experimentally observed lifetime is given in Fig. 5. The results show a reasonable agreement at lifetimes up to 10^4 cycles. At higher lifetimes the predicted values fall below the experimentally observed lifetimes. Deviations from the experimental data can mainly be attributed to the simplifications assumed in the model with respect to the microstructure. For example orientation differences from grain to grain and the grain size distribution are not taken into account.

In Fig. 6 the numerically adapted factor f is plotted as a function of the ratio of stress amplitude to cyclic yield strength for various materials. f can be interpreted as the degree of irreversibility of slip processes within the plastic zone. From this point of view an increase of f with increasing stress amplitude and decreasing cyclic strength seems to be reasonable, while the relative low values of f are somewhat surprising.

Conclusions

The low-cycle fatigue behaviour of Alloy 800H at room temperature has been studied with special emphasis on short crack growth behaviour. The main results can be summarized as follows:

1) The material reaches a stable saturation state (cyclic saturation) after having passed a relatively small stage of cyclic hardening at the beginning of cyclic deformation.
2) Crack growth studies indicate that the crack path and the crack propagation rate are strongly affected by the interaction of the crack with grain boundaries.
3) A crack growth model after Navarro et al. describing the crack propagation of short cracks was applied to the test results. The calculation provides limiting crack growth curves for the expected minimum and maximum crack growth rates.
4) The parameter f of the model, which represents the part of crack tip plastic displacement being converted into crack growth, increases with decreasing cyclic yield strength and increasing stress amplitude.
5) The cyclic lifetime was estimated by integrating the crack growth equation. The results show reasonable agreement with the experimental data. Only at cyclic lifetimes higher than 10^4 a very conservative prediction was found.

References

(1) Miller, K. J., Fatigue Fract. Engng. Mater. Struct., Vol. 10 , 1987, pp. 75-91
(2) Navarro, A., De Los Rios, E. R., Fatigue Fract. Engng. Mater. Struct., Vol. 11, 1988, pp. 383-396.
(3) Navarro, A., De Los Rios, E. R., Phil. Mag. A, Vol. 57, 1988, pp. 15-36.
(4) Navarro, A., De Los Rios, E. R., Phil. Mag. A, Vol. 57, 1988, pp. 37-42.
(5) Orr, J., in "Alloy 800", Edited by W. Betteridge, R. Krefeld, H. Kröckel, S. J. Lloyd, M. van de Voorde, C. Vivante, North Holland Pub. Co., Amsterdam, 1978, pp. 25-59.
(6) Nilsson, J.-O., Thorvaldsson, T., Fatigue Fract. Engng. Mater. Struct., Vol. 8, 1985 , pp. 373-384.
(7) Adolfs, R., Detert, K., in "Low Cycle Fatigue and Elasto-Plastic Behaviour of Materials-3", Edited by K.-T. Rie, Elsevier Applied Science, London , 1992, pp. 582-587.

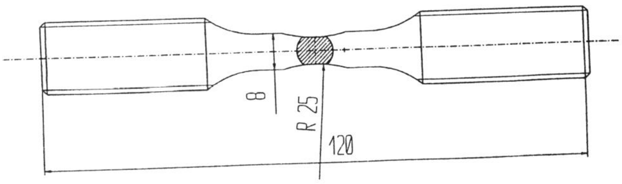

Figure 1. Geometry of the samples used for crack growth studies

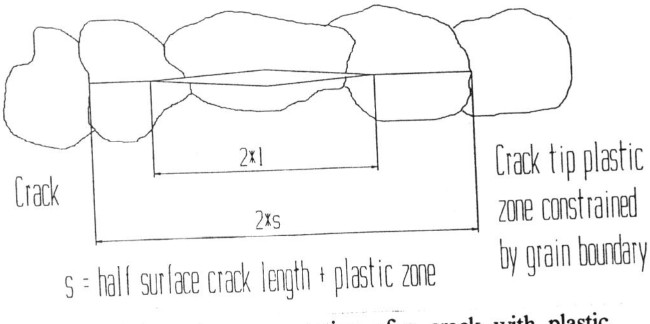

Figure 2. Schematic representation of a crack with plastic zones blocked at grain boundaries

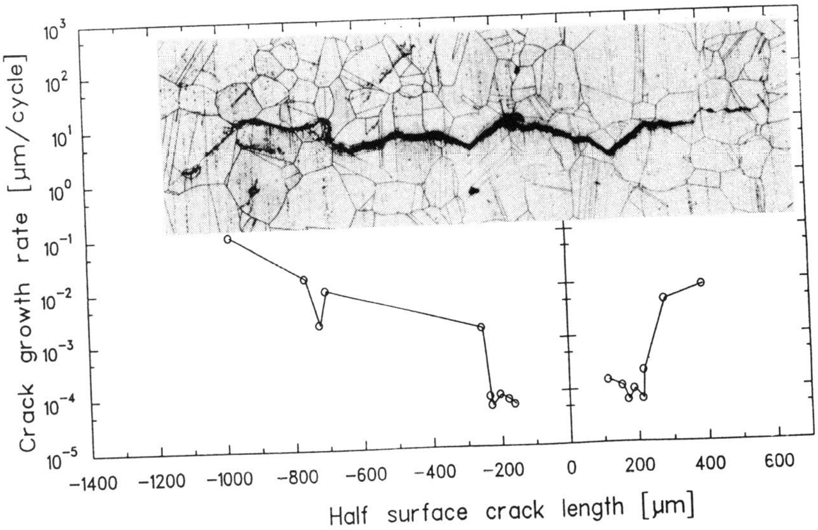

Figure 3. Crack growth rate as a function of surface crack length; the optical micrograph shows the corresponding fatigue crack

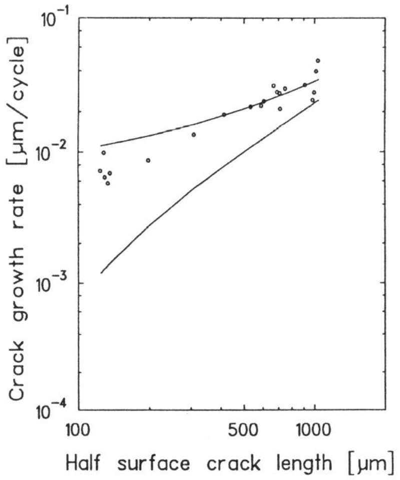

Figure 4. Comparison of calculated (solid lines) and measured crack growth rates

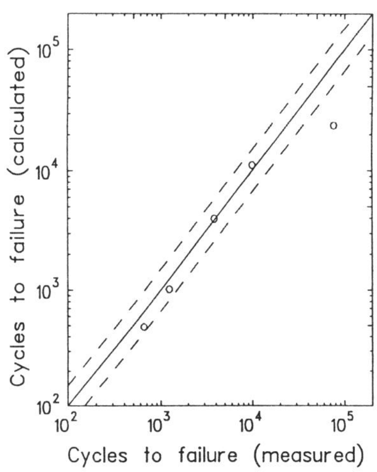

Figure 5. Comparison of predicted and observed cyclic lifetimes

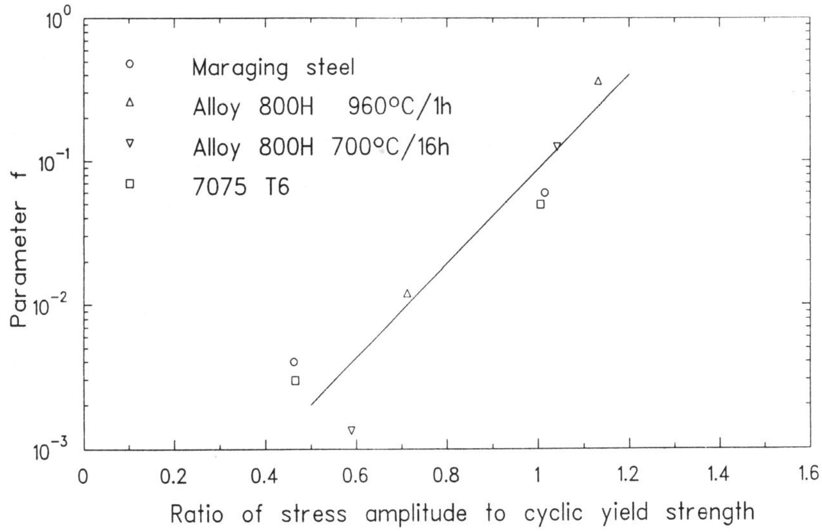

Figure 6. The value of parameter f as a function of the ratio of stress amplitude to cyclic yield strength plotted for various alloys